Supplementary Information

Water-soluble Terphen[3]arene Macrocycle: A Versatile Reversal Agent of Neuromuscular Blockers

Yibo Zhao,[a] Longming Chen,[b] Junyi Chem,[bc] Jian Li,[d] Qingbin Meng,[*b] Andrew C.-H. Sue[*a] and Chunju Li[*b]

a. School of Pharmaceutical Science and Technology, Tianjin University, Tianjin 300387 P. R. China.

b. State Key Laboratory of Toxicology and Medical Countermeasures, Beijing Institute of Pharmacology and Toxicology, Beijing 100850, P. R. China.

c. Tianjin Key Laboratory of Structure and Performance for Functional Molecules, College of Chemistry, Tianjin Normal University, Tianjin 300387 P. R. China.

d. School of Chemistry and Chemical Engineering, Henan Normal University, P. R. China.

Table of Contents

1. General materials and methods

1.1. Materials and instruments

All the reagents and solvents were commercially available and used as received unless other specified purification. Dulbecco's modified eagle medium (DMEM) was purchased from Gibco (Thermo Fisher Scientific). Fetal bovine serum (FBS), penicillin-streptomycin and PBS were purchased from Invitrogen (Carlsbad, CA, USA). The human normal renal epithelial cells (293T) was purchased from Cell Resource Center (Beijing, China).

NMR date were recorded on a Bruker Advance 400/600 MHz spectrometers at room temperature, unless otherwise noted. The chemical shifts in NMR spectra are reported in ppm proton resonance resulting from incomplete deuteration of the NMR solvents. High-resolution electrospray ionization (HR-ESI) mass spectral analyses were performed by the Thermo Fisher Q Exactive™ HF/UltiMate™ 3000 RSLCnano. Fluorescence emission spectra was recorded on an Edinburgh Instruments FLS980 time-resolved fluorescence spectrometer equipped with an integrating sphere. Cytotoxicity studies were performed on SpectraMax ® M5 plate reader, Molecular Devices. The muscle relaxation mouse model was recorded using the YSL-4C Rota-rod rotor.

1.2. Cell and animals

293T cells were cultured in DMEM supplemented with 10% FBS, 1% penicillin and 1% streptomycin. Then cells were incubated at 37 ^{o}C under 5% CO_2 and 90% relative humidity, and passaged every 2 days. KM mice with 18-22 g weight were purchased from the SPF Biotechnology Co. Ltd and approved by Beijing Institute of Pharmacology and Toxicology. All mice have free access to food and water throughout the experiments. All animal experiments meet the requirements of the ethical review committee. The animal experiments were approved by the Institutional Animal Care and Use Committee of the Center, which followed the guidelines of the Association for Assessment and Accreditation of Laboratory Animal Care International (AAALAC).

1.3. Fluorescence titration[1]

To quantitatively assess the complexation behavior of **NMBAs** and **WTP3**, fluorescence titrations of hosts with guests were performed at 298 K in a phosphate buffer solution of pH 7.4 by equation 1. We considered that a guest formed a 1:1 host:guest complex with a host at an

association constant (K_a), which satisfied the respective law of mass action relating to the equilibrium concentrations of free host ([H]), free guest ([G]) and host-guest complex ([HG]). The relationship between the total concentration of host ($[H]_0$), guest ($[G]_0$) and their equilibrium concentrations were introduced by the law of mass conservation (equation 2-1 and 2-2). Here $[G]_0$ was the initial concentration of guest as a known parameter, which was kept constant in the titration process. Then equation 1 and 2-2 were employed to deduced equation 3. When the fluorescence titration was performed, the intensity of fluorescence (F) corresponded to the combined intensity of the host and the host-guest complex, which were described by molar fractions (equation 4). Both F_{HG} and F_G were known parameters in which F_G was the fluorescent of $[G]_0$ and F_{HG} was the fluorescent intensity when all guests were complexed. The equation 5 deduced by equation 2-1, 2-2, 3 and 4, explained the relationship between K_a and variables $[H]_0$ in fluorescence titration.

$$[H] + [G] \overset{K_a}{\leftrightarrow} [HG]$$

$$K_a = \frac{[HG]}{[H][G]} \tag{1}$$

$$[G] = [G]_0 - [HG] \tag{2-1}$$

$$[H] = [H]_0 - [HG] \tag{2-2}$$

$$[HG] = \frac{K_a[H][G]_0}{1 + K_a[H]} \tag{3}$$

$$F = \frac{[HG]}{[G]_0}F_{HG} + \frac{[G]}{[G]_0}F_G \tag{4}$$

$$F = F_{HG} + (F_G - F_{HG})\frac{\left([G]_0 - [H]_0 - \frac{1}{K_a}\right) - \sqrt{\left([G]_0 - [H]_0 - \frac{1}{K_a}\right)^2 + 4[H]_0[G]_0}}{2G_0} \tag{5}$$

To proceed the competitive titrations, we considered competitors that could competitively bind to host in a 1:1 stoichiometry at an association constant (K_c, equation 6). Free host (H), free competitor (C) and host-competitor complex (HC) obeyed the respective law of mass action referring to equilibrium concentrations. Here the total concentration of host ($[H]_0$), competitor ($[C]_0$) and their equilibrium concentrations satisfied the law of mass conservation (equation 7). In the course of titration, the fluorescence intensity (F_C) was expressed as a linear combination of F_{HG} and F_G, weighted by their molar fractions on the basis of equation 8. Through a 1:1 host-guest

binding model, F_{HG} was the initial experimental fluorescence intensity in the absence of C. Substituting equation 3 into equation 8 gave equation 9, with the concentration of uncomplexed host as an unknown parameter ([H]), which was numerically solved by equation 10. Note: equation 10 was deduced by combination equation 3, 6, 7-1 and 7-2. For fitting, the fluorescence intensity was plotted against $[C]_0$ based on equation 9.

$$[H] + [G] \overset{K_c}{\leftrightarrow} [HG]$$

$$K_c = \frac{[HC]}{[H][C]} \tag{6}$$

$$[H] = [H]_0 - [HG] - [HC] \tag{7-1}$$

$$[C] = [C]_0 - [HC] \tag{7-2}$$

$$F_C = \frac{[HG]}{[G]_0} + \frac{[G]}{[G]_0} F_G \tag{8}$$

$$F_C = F_G + (F_{HG} - F_G) \frac{K_a[H]}{1 + K_a[H]} \tag{9}$$

$$0 = A[H]^3 + B[H]^2 + C[H] + D$$
$$A = K_a K_C$$
$$B = K_a + K_C + K_a K_C([G]_0 + [C]_0 - [H]_0)$$
$$C = K_C([C]_0 - [H]_0) - K_a([H]_0 - [G]_0) + 1$$
$$D = -[H]_0 \tag{10}$$

1.4. Synthetic procedures of container **WTP3**

The first compounds **TP3** were synthesized by using the method from the reference.[2]

Synthesis of TP3-OH. To solution of **TP3** (490.00 mg, 0.45mmol) in 150.00 mL DCM and replace argon three times. Put the flask in ice bath and dropwise boron tribromide (1.30 mL, 135.00 mmol) into reaction solution slowly. The resulting mixture was stirred under Ar for 18 hours. Add ice water to quench the reaction. The product was extracted with ethyl acetate for three time. Combine the organic phase, and dried to afford a light yellow solid (392.85 mg, 0.43 mmol, 95% yield). The product **TP3-OH** was proceeded directly to the next reaction. ^{1}H NMR (400 MHz, acetone-d_6) δ (ppm): 7.49 (s, 12H), 7.16 (s, 6H), 6.55 (s, 6H), 3.89 (s, 6H). ^{13}C NMR (100 MHz, acetone-d_6) δ (ppm): 155.1, 154.2, 137.4, 132.8, 129.5, 121.5, 120.3, 104.2.

Synthesis of WTP3. To a mixture of **TP3-OH** (140.00 mg, 0.15 mmol) and pyridine sulfur trioxide complex (716.22 mg, 4.50 mmol) was added dry pyridine (10.00 mL). The resulting mixture was stirred at 75 °C under Ar for 12 hours. The reaction mixture was allowed to cool to

RT and pyridine poured out. The crude solid was washed by dichloromethane and ethyl acetate for two times. Then, adjusted to pH = 7.5 by slow addition of saturated aqueous $NaHCO_3$. After addition of EtOH (30.00 mL), the crude product was collected by centrifugation 3500 rpm × 10 min. The precipitate was suspended in ethanol (30.00 mL × 2), sonicated for 3 minutes, and solid collected by centrifugation. The crude solid was redissolved in MeOH. Desalination by centrifugation. After drying under high vacuum, **WTP3** was obtained as a light yellow solid (273.29 mg, 0.13 mmol, 82% yield). M.p. > 290 ˚C (decomposed). ^{1}H NMR (400 MHz, D_2O) δ (ppm): 7.66 (s, 6H), 7.53 (s, 12H), 7.28 (s, 6H), 4.11 (s, 12H). ^{13}C NMR (100 MHz, D_2O and 1% CD_3OD) δ (ppm): 149.0, 146.9, 136.0, 132.0, 131.0, 139.2, 115.0. HR-MS (ESI): m/z 1047.7796 ($C_{57}H_{30}Na_{10}O_{48}S_{12}^{2-}$), calculated 1047.7772; 690.8562 ($C_{57}H_{30}Na_9O_{48}S_{12}^{3-}$), calculated 690.8550; 512.3943 ($C_{57}H_{30}Na_8O_{48}S_{12}^{4-}$), calculated 512.3940.

1.5. Molecular docking model

Three-dimensional structures of these NMBAs and container **WTP3** were drawn with ChemBioDraw Ultra 14.0 software. AutoDock Tools-1.5.6 was used to generate the pdb (protein data bank) files. The binding model of **NMBAs**/**WTP3** were simulated with AutoDock Vina. A grid map of dimensions 18 Å × 14 Å × 14 Å with a grid space of 1.000 Å was set. The center of the search space was set to 0.221 Å, 0.000 A and 0.000 Å (x, y, z).

1.6. In vitro cytotoxicity studies

The relative cytotoxicity of **WTP3** against 293T cells were assessed in vitro using CCK-8 according to the manufacture's instruction. 293T cells were seeded into 96-well plates at a density of 8000 cells/well in 100 μL of DMEM supplemented with 10% FBS, 1% penicillin, and 1% streptomycin and cultured for 24 h in 5% CO_2 at 37 °C. **WTP3** was dissolved in PBS and then diluted to the required concentration. It was then added to the cell-containing wells which were further incubated at 37 °C under 5% CO_2 for 48 h. Subsequently, 10 μL of CCK-8 was added into each well and incubated for another 0.5 h. The plates were then measured at 450 nm using a plate reader. All experiments were carried out five independent times.

1.7. Locomotion recovery from muscle relaxation

The rotor parameter was set to 40 revolution per minute (rpm). KM mice were trained on the Rota-rod rotor five times a day by 20 minutes for two consecutive days in advance, and each training time was 20 minutes. The mice were chosen that would not fall from the YLS-4C within 30 s and randomly divided into three groups with 10 mice in each group. The mice could not move on the rotor for 30 s showed that a mouse model of muscle relaxation was established successfully according to previously reported.[3] We start the timer, when intravenous injection of 0.40 mg/kg of **Cis** is finished and end the timer when the mice could move on the rotor for 30 s continuously. One minute after injection of **Cis**, the mice were administered with either PBS or 0.69 mg/kg of **WTP3** and their locomotion behaviours were immediately monitored (The administration volumes of **Cis** and **WTP3** are both 10 mL/kg).

2. Supporting results and experimental raw data

2.1. Characterization of **WTP3** and host-guest complex

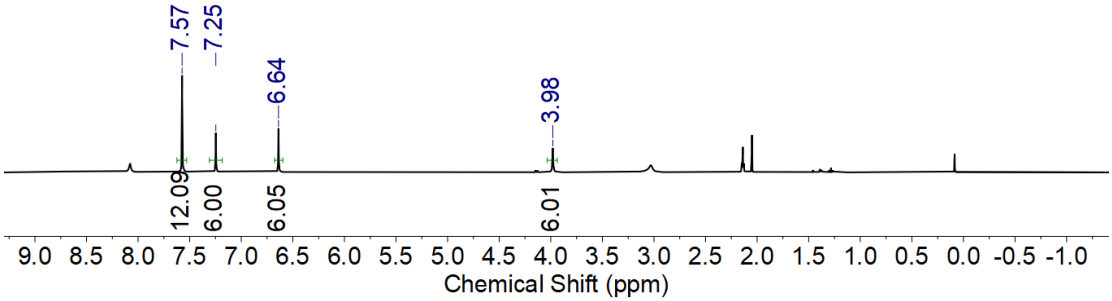

Fig. S1. ^{1}H NMR spectrum (400 MHz, Acetone-d_6, 298 K) of **TP3-OH**.

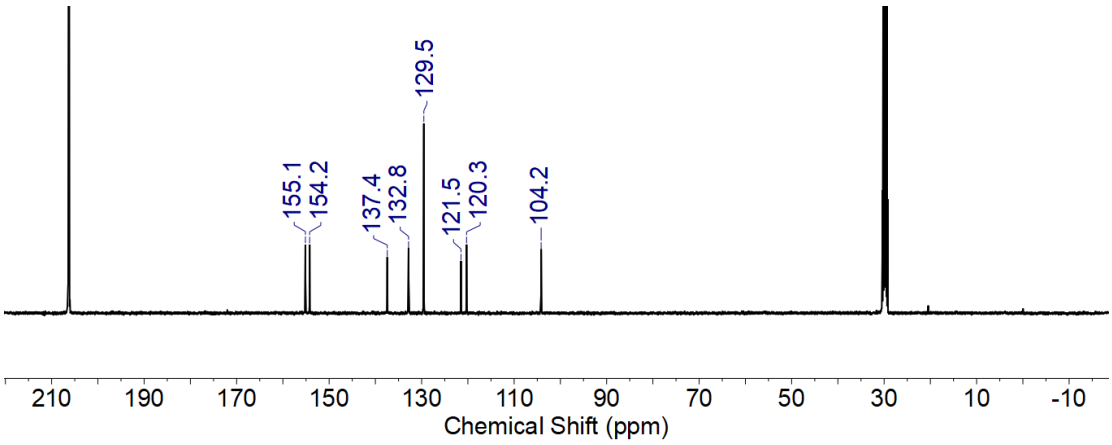

Fig. S2. ^{13}C NMR spectrum (400 MHz, Acetone-d_6, 298 K) of **TP3-OH**.

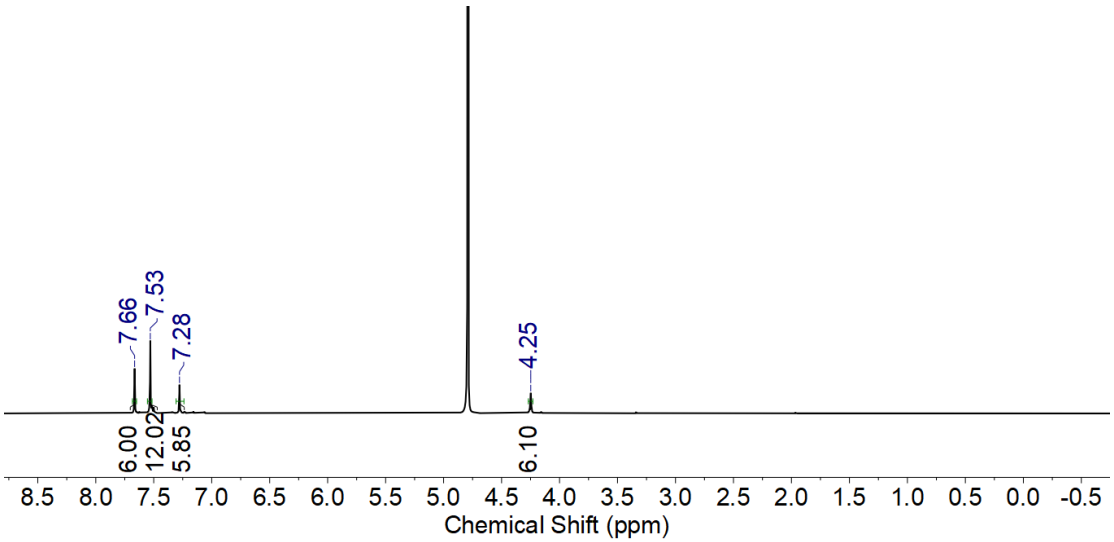

Fig. S3. ^{1}H NMR spectrum (400 MHz, D_2O, 298 K) of **WTP3**.

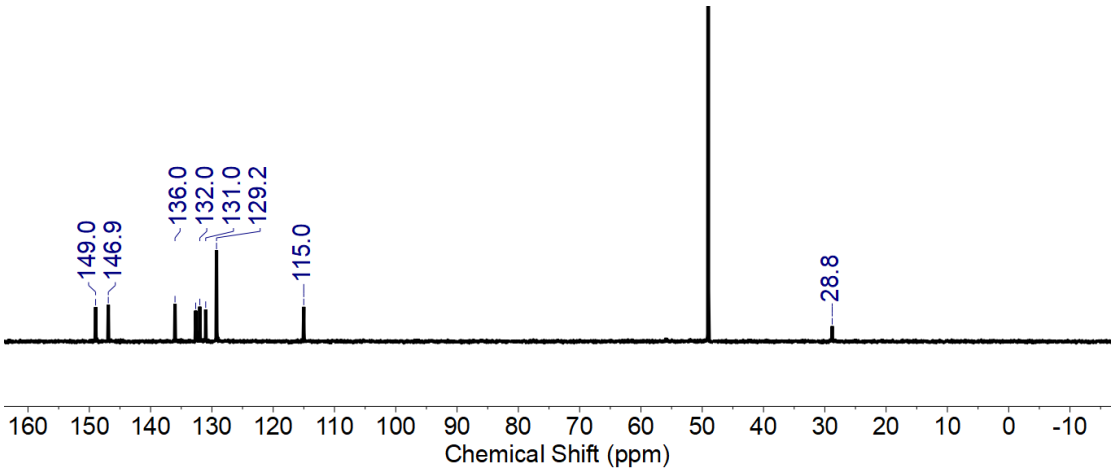

Fig. S4. ^{13}C NMR spectrum (400 MHz, D_2O with 1% CD_3OD as interior label, 298 K) of **WTP3**.

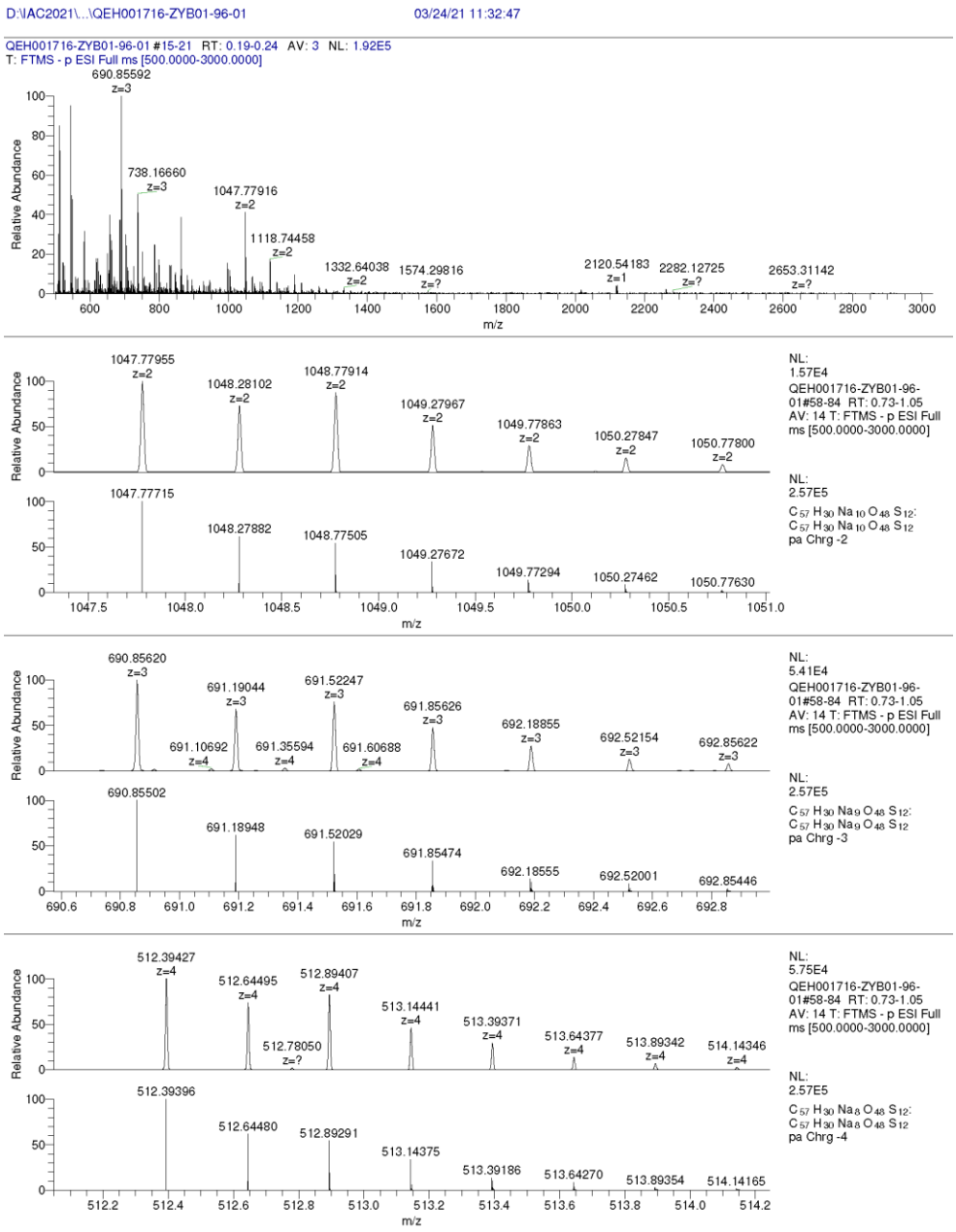

Fig. S5. ESI-MS spectra of **WTP3**.

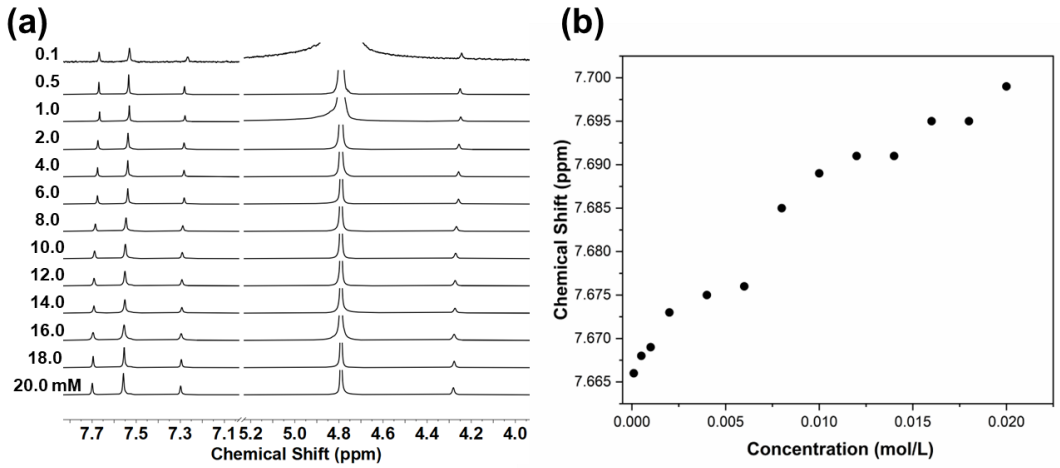

Fig. S6. (a) ^{1}H NMR spectra (400 MHz, D_2O, 298K) recorded for the dilution of container **WTP3** (20.0 - 0.1 mM). **WTP3** itself weakly self-associated in water, which is evidenced by the upfield chemical shift changes of the aromatic region at 7.67 – 7.70 ppm protons. (b) Plot of chemical shift of **WTP3** versus [**WTP3**].

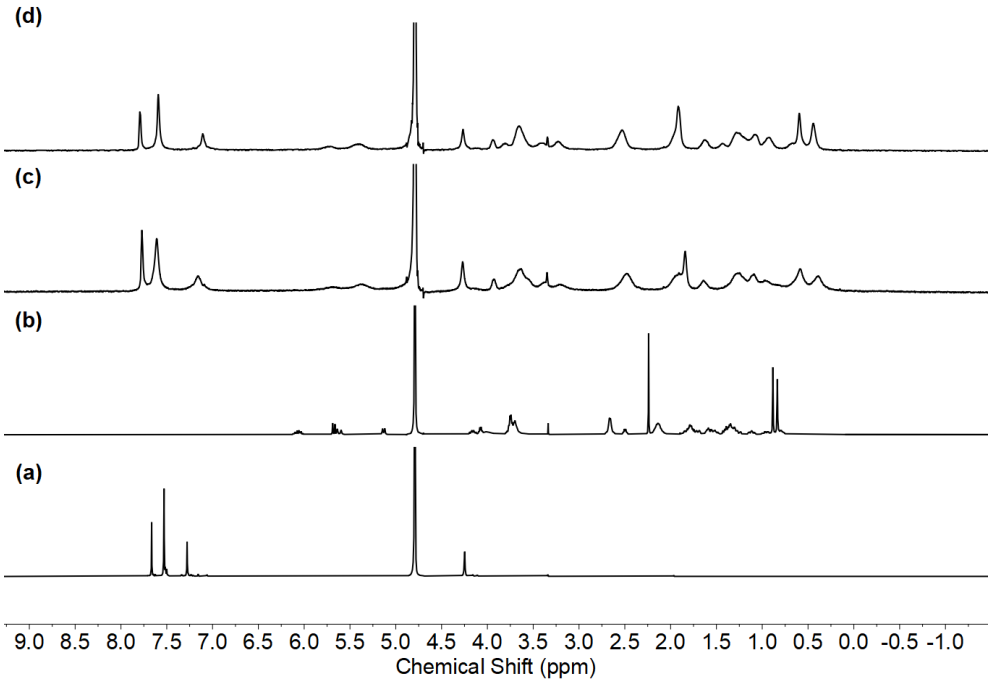

Fig. S7. ^{1}H NMR spectrum recorded (400 MHz, D_2O, 298 K) for: (a) **WTP3** (5.0 mM), (b) **Roc** (5.0 mM), (c) **Roc/WTP3** complex (2.5 mM), and (d) a mixture of **Roc/WTP3** (1.3 mM) and excess **Roc** (3.3 mM).

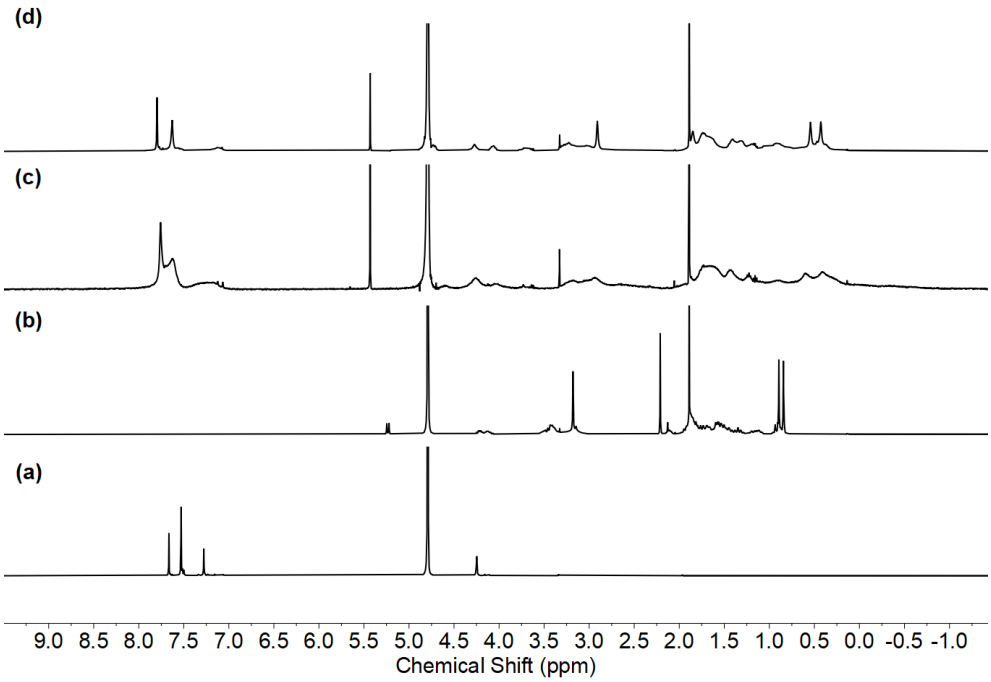

Fig. S8. ^{1}H NMR spectrum recorded (400 MHz, D_2O, 298 K) for: (a) **WTP3** (5.0 mM), (b) **Vec** (5.0 mM), (c) **Vec/WTP3** complex (2.5 mM), and (d) a mixture of **Vec/WTP3** (1.3 mM) and excess **Vec** (3.3 mM).

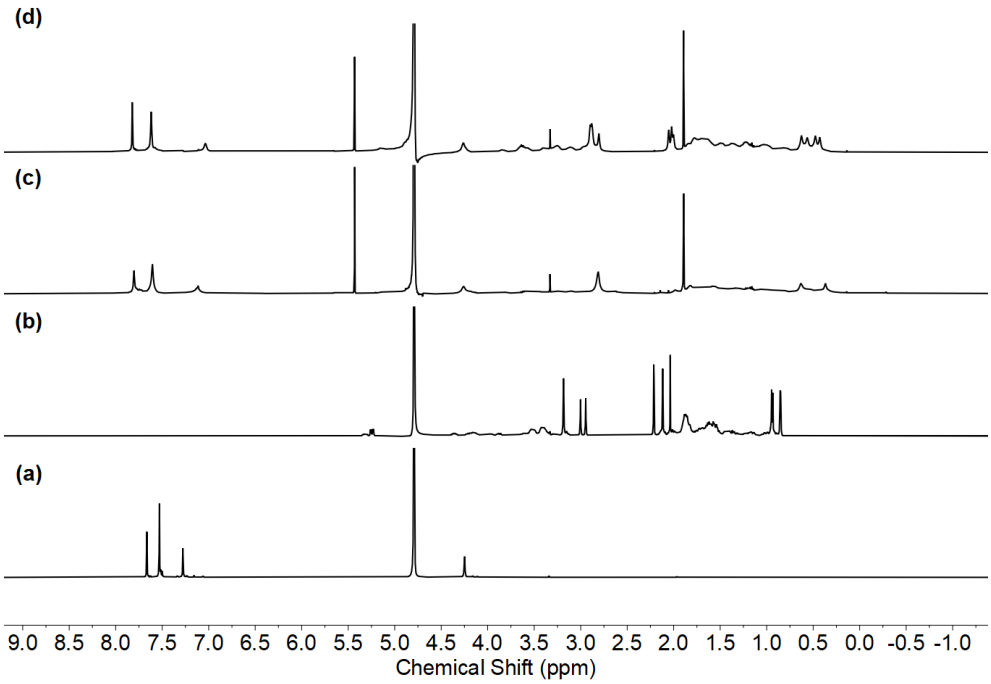

Fig. S9. ^{1}H NMR spectrum recorded (400 MHz, D_2O, 298 K) for: (a) **WTP3** (5.0 mM), (b) **Pan** (5.0 mM), (c) **Pan/WTP3** complex (2.5 mM), and (d) a mixture of **Pan/WTP3** (1.3 mM) and excess **Pan** (3.3 mM).

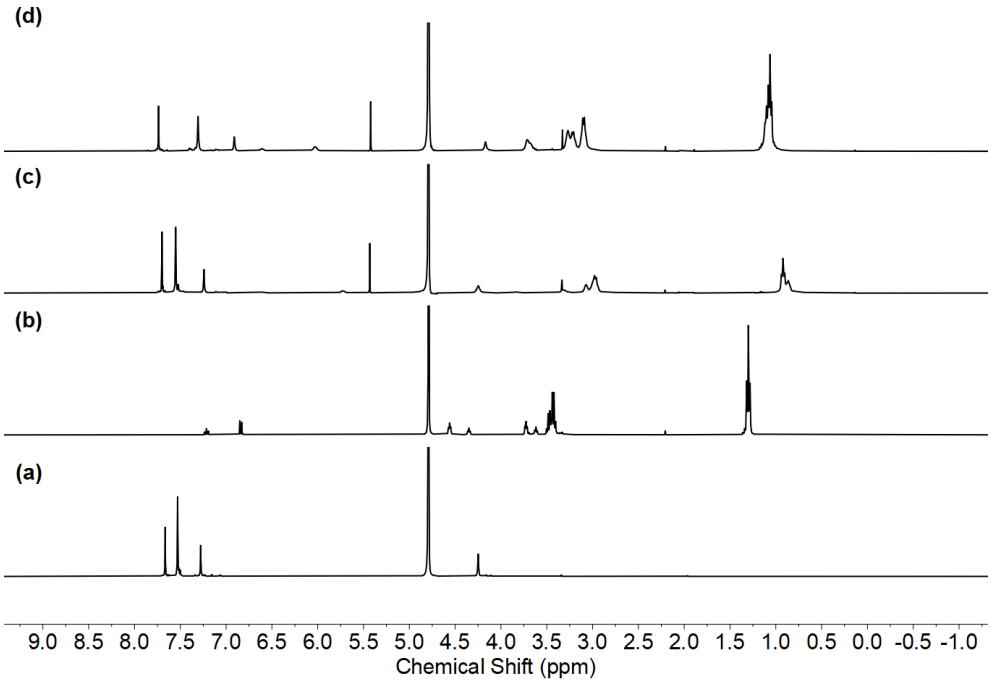

Fig. S10. ^{1}H NMR spectrum recorded (400 MHz, D_2O, 298 K) for: (a) **WTP3** (5.0 mM), (b) **Gal** (5.0 mM), (c) **Gal/WTP3** complex (2.5 mM), and (d) a mixture of **Gal/WTP3** (1.3 mM) and excess **Gal** (3.3 mM).

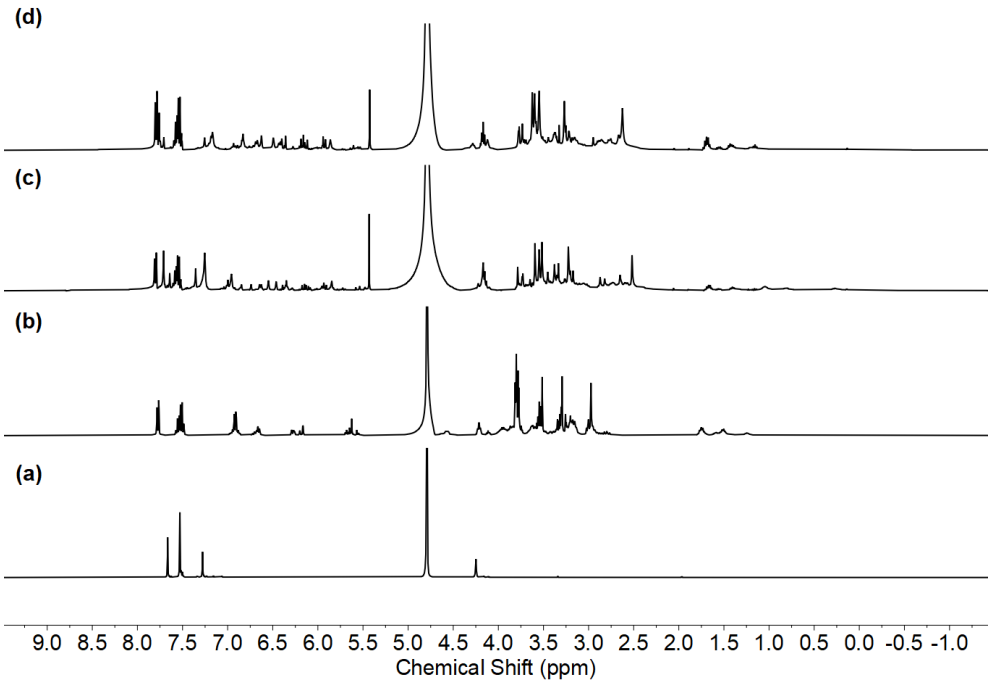

Fig. S11. ^{1}H NMR spectrum recorded (400 MHz, D_2O, 298 K) for: (a) **WTP3** (5.0 mM), (b) **Cis** (5.0 mM), (c) **Cis/WTP3** complex (2.5 mM), and (d) a mixture of **Cis/WTP3** (1.3 mM) and excess **Cis** (3.3 mM).

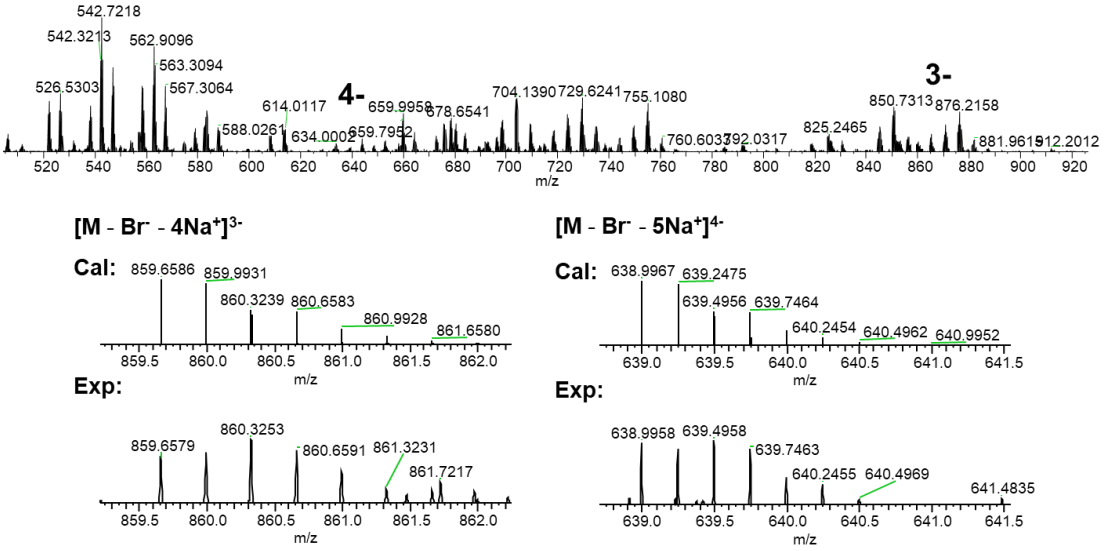

Fig. S12. ESI-MS spectra of **Roc/WTP3**.

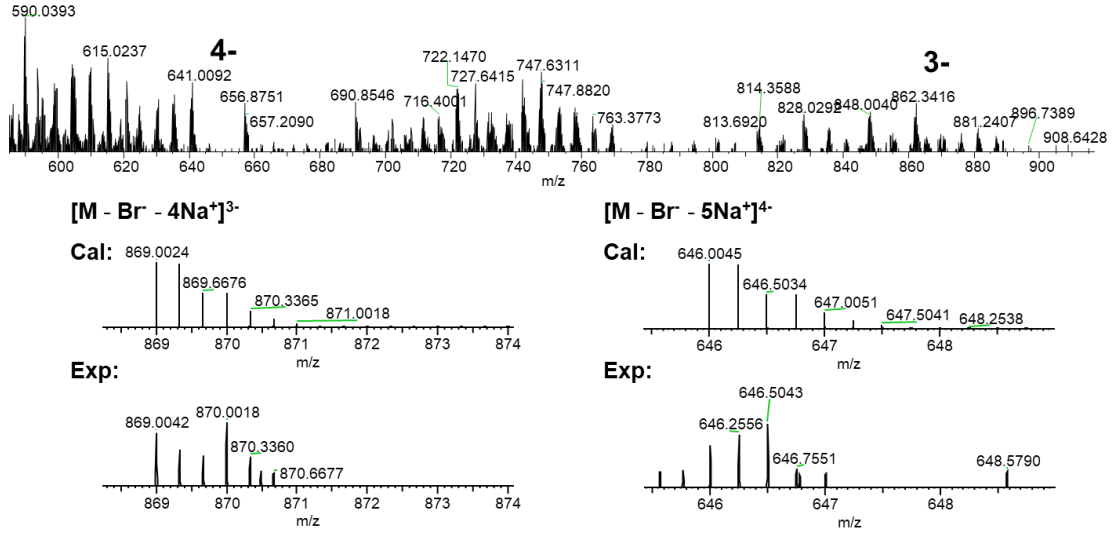

Fig. S13. ESI-MS spectra of **Vec/WTP3**.

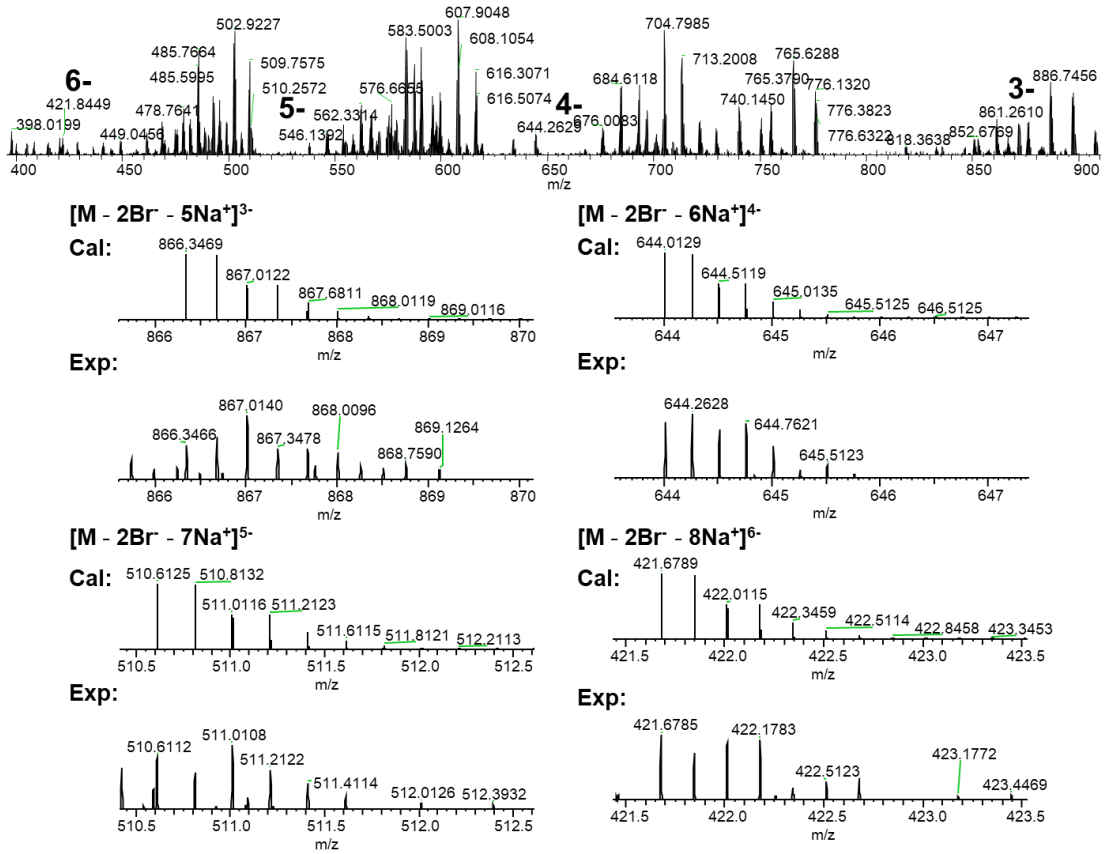

Fig. S14. ESI-MS spectra of **Pan/WTP3**.

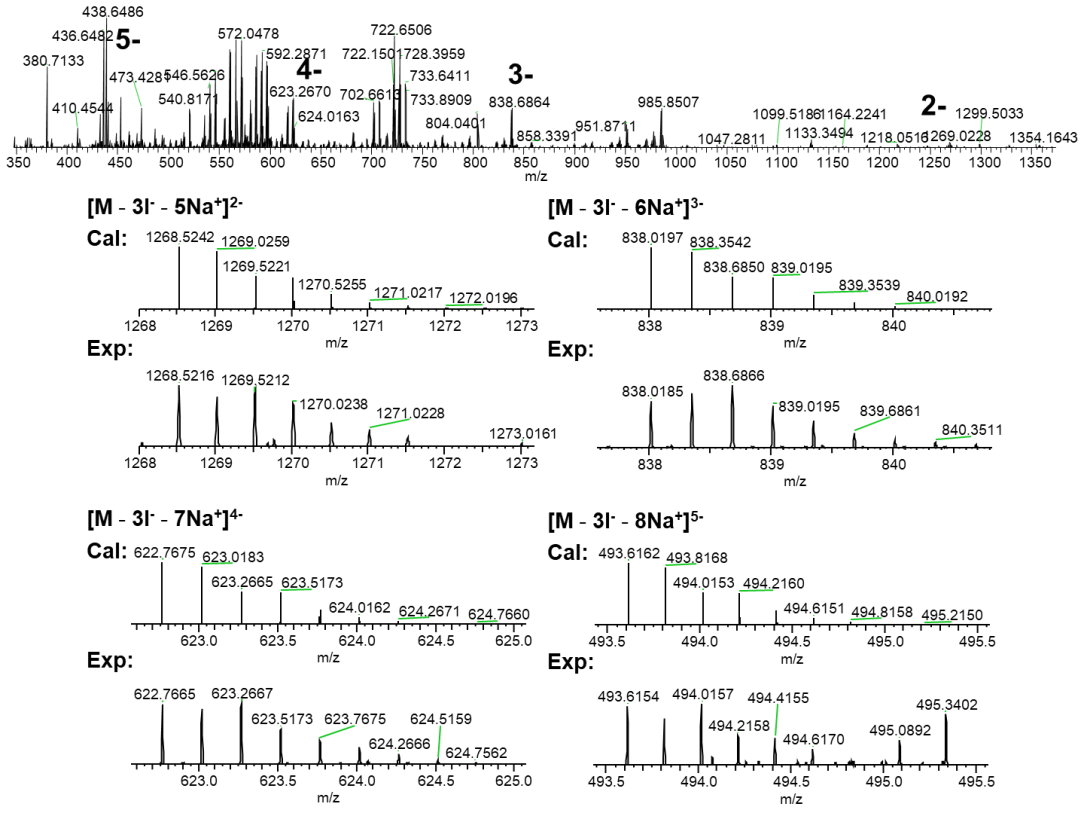

Fig. S15. ESI-MS spectra of **Gal/WTP3**.

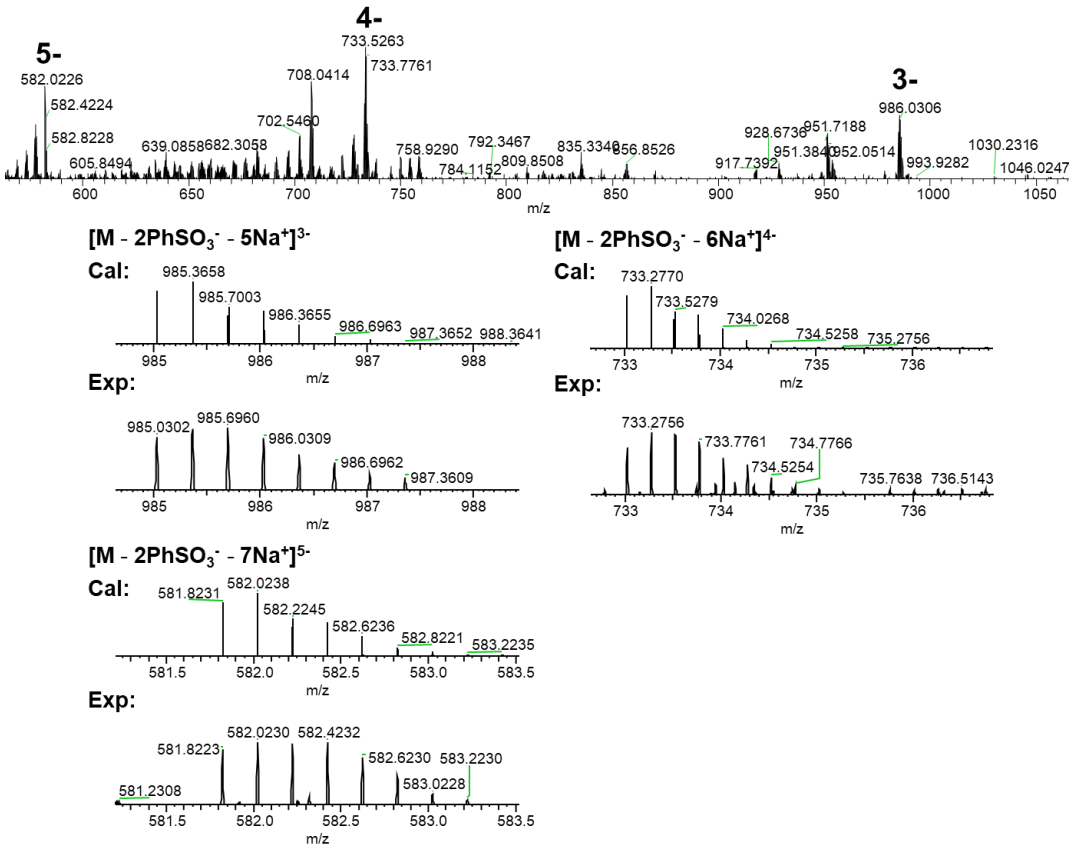

Fig. S16. ESI-MS spectra of **Cis/WTP3**.

2.2. Structural presentation of **NMBA/WTP3**

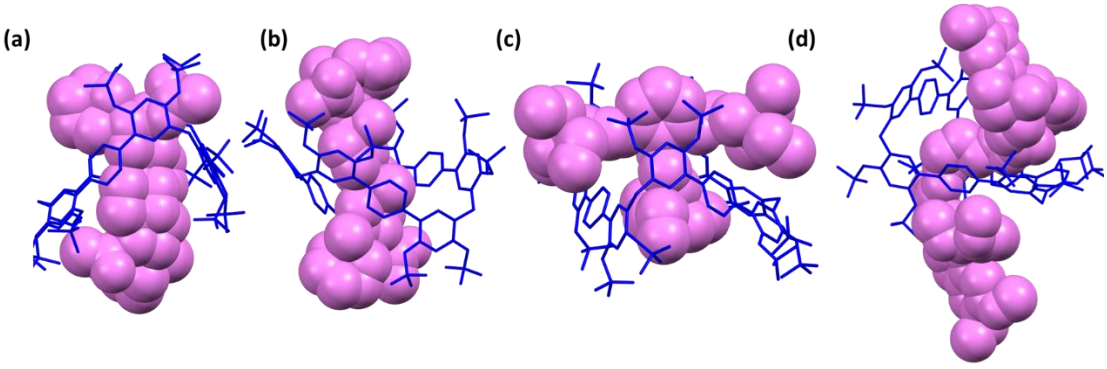

Fig. S17. Molecular docking simulation of (a) **Vec/WTP3**, (b) **Pan/WTP3**, (c) **Gal/WTP3** and (d) **Cis/WTP3** complexes in aqueous solution.

2.3. Job's plot analysis for complexation of **Rho123** with **WTP3**

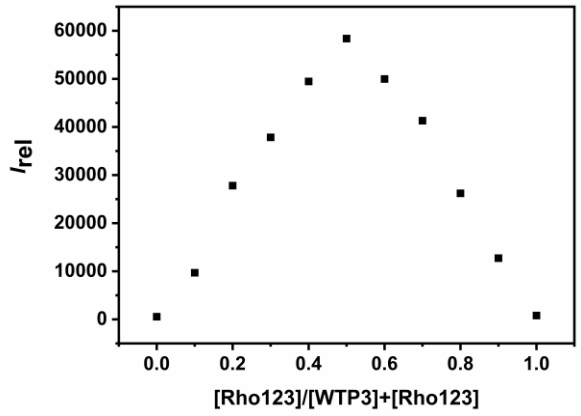

Fig. S18. Job's plot for **WTP3** with **Rho123** in 10 mM PBS buffer at pH 7.4 (λ_{ex} = 329 nm, λ_{em} = 526 nm, [**WTP3**] + [**Rho123**]) = 1.0 μM).

2.4. Binding affinities between container **WTP3** and different NMBAs guests

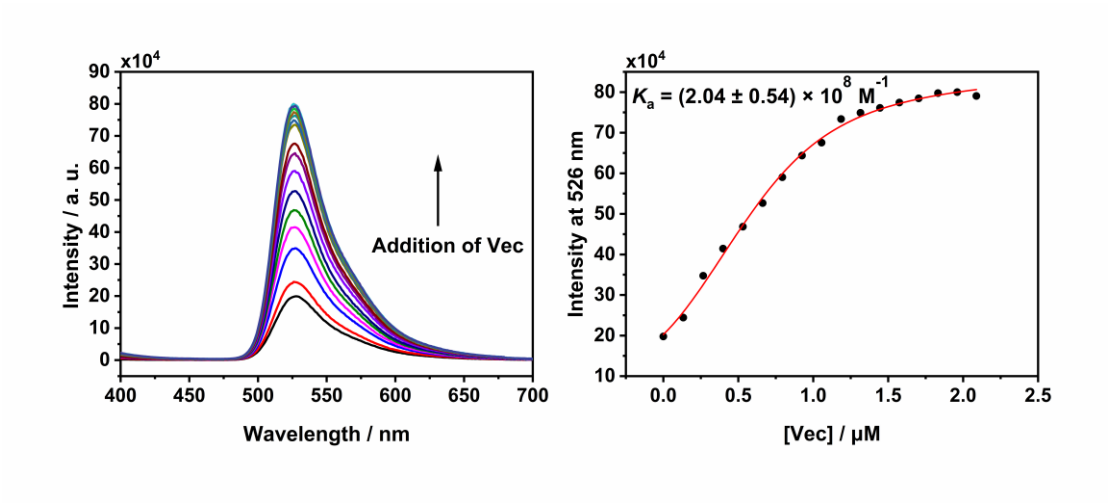

Fig. S19. (a) Competitive fluorescence titration of **Vec** in presence of **Rho123@WTP3**. (b) The associated titration curve. Competitive fluorescence titration of **Vec** in presence of **Rho123@WTP3** (1.0/1.0 μM) in PBS buffer (10 mM, pH = 7.4) and λ_{ex} = 329 nm. The associated titration curve at λ_{em} = 526 nm and fit according a 1:1 competitive binding model. All date are from n = 3 independent experiments and are presented as mean ± SD.

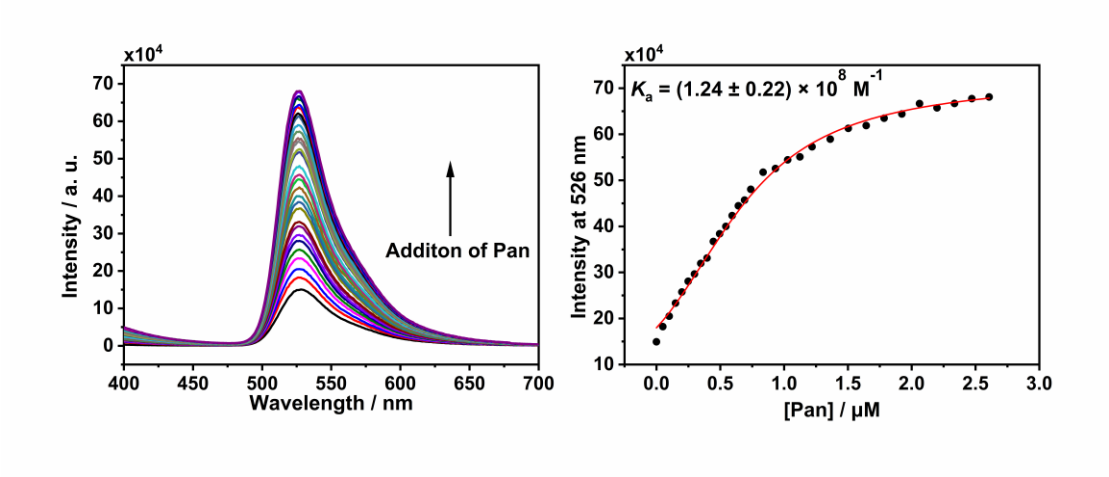

Fig. S20. (a) Competitive fluorescence titration of **Pan** in presence of **Rho123@WTP3**. (b) The associated titration curve. Competitive fluorescence titration of **Pan** in presence of **Rho123@WTP3** (1.0/1.0 μM) in PBS buffer (10 mM, pH = 7.4) and λ_{ex} = 329 nm. The associated titration curve at λ_{em} = 526 nm and fit according a 1:1 competitive binding model. All date are from n = 3 independent experiments and are presented as mean ± SD.

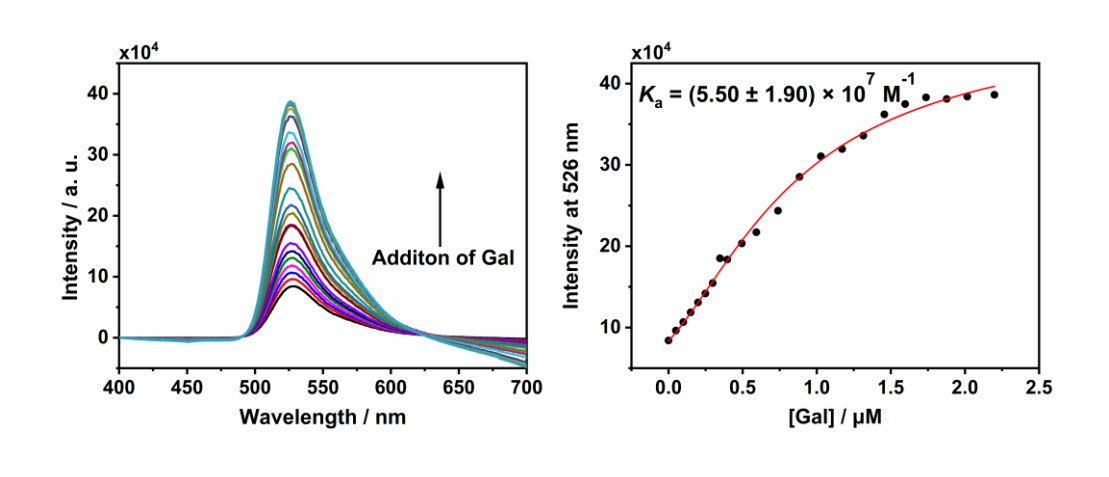

Fig. S21. (a) Competitive fluorescence titration of **Gal** in presence of **Rho123@WTP3**. (b) The associated titration curve. Competitive fluorescence titration of **Pan**, **Gal** in presence of **Rho123@WTP3** (1.0/1.0 μM) in PBS buffer (10 mM, pH = 7.4) and λ_{ex} = 329 nm. The associated titration curve at λ_{em} = 526 nm and fit according a 1:1 competitive binding model. All date are from n = 3 independent experiments and are presented as mean ± SD.

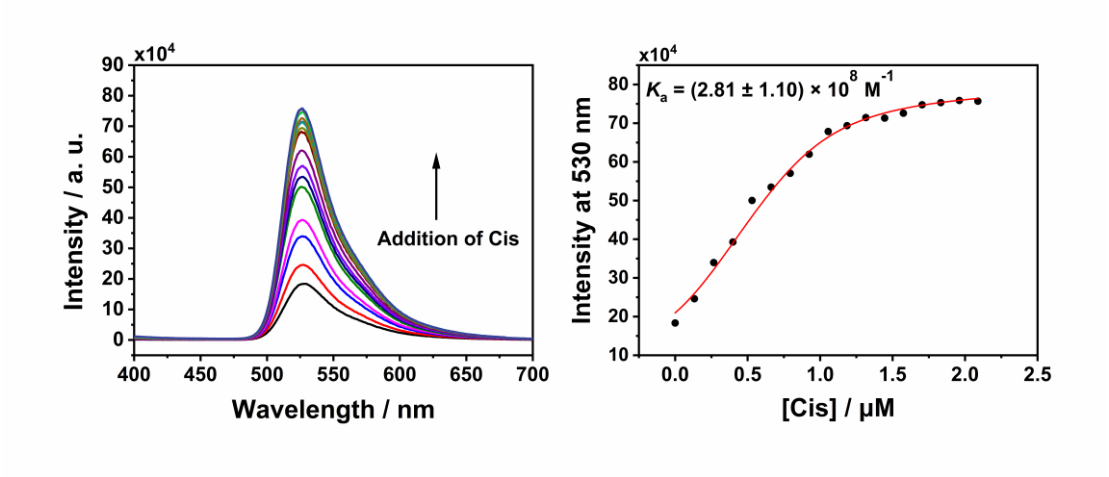

Fig. S22. (a) Competitive fluorescence titration of **Cis** in presence of **Rho123@WTP3**. (b) The associated titration curve. Competitive fluorescence titration of **Cis** in presence of **Rho123@WTP3** (1.0/1.0 μM) in PBS buffer (10 mM, pH = 7.4) and λ_{ex} = 329 nm. The associated titration curve at λ_{em} = 530 nm and fit according a 1:1 competitive binding model. All date are from n = 3 independent experiments and are presented as mean ± SD.

2.5. The fluorescence responses of **Rho123/WTP3** towards **Cis** and some biologically important species

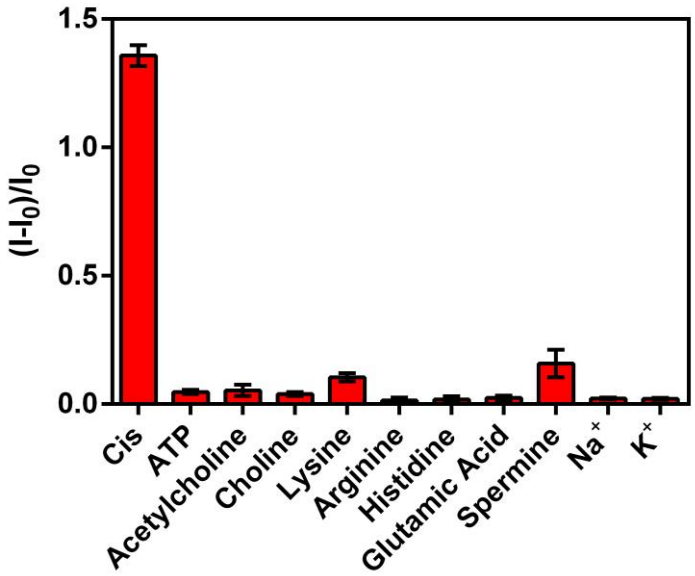

Fig. S23. Fluorescence responses of **Rho123** (1.00 μM)/**WTP3** (1.00 μM) at 525 nm (λ_{ex} = 500 nm) upon addition of **Cis** and various biological co-existing species (20 μM) in PBS buffer. Data were from n = 3 independent experiments and are presented as mean ± SD.

Reference:

[1] (a) A. Henning, H. Bakirci, W. M. Nau, *Nat. Methods*, **2007**, 4, 629-632. (b) G. Ghale, W. M. Nau, *Acc. Chem. Res.*, **2014**, 47, 947-955. (c) R. N. Dsouza, U. Pischel, W. M. Nau, *Chem. Rev.*, **2011**, 111, 7941-7980.

[2] K.-D. Xu, Z.-Y. Zhang, C.-M. Yu, B. Wang, M. Dong, X.-Q. Zeng, R. Gou, L. Cui, C.-J. Li, *Angew. Chem. Int. Ed.*, **2020**, 59, 7214-7218.

[3] X.-J. Zhang, Q.-C. Cheng, L.-L. Li, L.-Q. Shangguan, C.-W. Li, S.-K. Li, F.-H. Huang, J.-X. Zhang, R.-B. Wang, *Theranostics*, **2019**, 9, 3107-3121.